In Silico Design of DNP Polarizing Agents:

Can Current Dinitroxides be Improved?

Frédéric A. Perras,[a] Aaron Sadow,[a,b] Marek Pruski[a,b]*

[a] US DOE, Ames Laboratory, Ames, IA, 50011, USA

[b]Department of Chemistry, Iowa State University, Ames, IA, 50011, USA

*Corresponding author: mpruski@iastate.edu

Abstract

Numerical calculations of enhancement factors offered by dynamic nuclear polarization in solids under magic angle spinning (DNP-MAS) were performed to determine the optimal EPR parameters for a dinitroxide polarizing agent. We found that the DNP performance of a biradical is more tolerant to the relative orientation of the two nitroxide moieties than previously thought. Generally, any condition in which the g_{yy} tensor components of both radicals are perpendicular to one another is expected to have near-optimal DNP performance. Our results highlight the important role of the exchange coupling, which can lessen the sensitivity of DNP performance to the inter-radical distance, but also lead to lower enhancements when the number of atoms in the linker becomes less than three. Lastly, the calculations showed that the electron T_{1e} value should be near 500 μs to yield optimal performance. Importantly, the newest polarizing agents already feature all of the qualities of the optimal polarizing agent, leaving little room for further improvement. Further research into DNP polarizing agents should then target non-nitroxide radicals, as well as improvements in sample formulations that target high-temperature DNP and limit quenching and reactivity.

Keywords

Dynamic Nuclear Polarization, Solid-State NMR, MAS-DNP, Dinitroxides, Simulations

Introduction

Applications of nuclear magnetic resonance (NMR) spectroscopy have always been restricted by the intrinsically low Boltzmann polarization of the nuclear magnetic eigenstates whose energy differences are at the lowest-energy end of the electromagnetic spectrum (i.e. radio frequencies). Consequently, large sample quantities and long acquisition times are needed to acquire the data. Additionally, in many fields such as materials chemistry and heterogeneous catalysis, model systems that approximate the more complex structures of dilute, industrially relevant materials, are often used. Clearly, the sensitivity of NMR spectroscopy needs to be improved in order to tackle the difficult problems related to the structures of such materials.[1],[2],[3],[4]

While other conventional means for sensitivity improvement, namely reducing the sample temperature and increasing the magnetic field strength to increase polarization[5] or cryogenically cooling the electronics to reduce noise,[6] have been thoroughly studied and applied, none of these approaches rival the sensitivity improvement afforded by hyperpolarization of nuclear spins. In particular, dynamic nuclear polarization (DNP) is rapidly becoming the hyperpolarization method of choice for NMR spectroscopy due to its ease of implementation and the generality of the technique.[7],[8],[9],[10] In a typical magic-angle spinning (MAS) DNP NMR experiment,[10],[11],[12],[13] the sample is first impregnated with a stable radical-containing solution; then, high-power microwaves, usually produced using a gyrotron,[14],[15] irradiate the sample near the electron Larmor frequency to transfer the high electron polarization to the nuclear spins. These experiments are typically performed at temperatures near 100 K. In theory, NMR sensitivity enhancements equaling the ratio of the electronic and nuclear magnetogyric ratios (γ_e/γ_n) can be obtained, corresponding to ~660 and ~4850 for ^{1}H and ^{17}O,

respectively, yet our abilities to reach such large enhancement factors have been limited by the intrinsic inefficiencies of the polarization transfer, stemming largely from the properties of radical polarizing agents.

The vast majority of DNP polarizing agents currently in use are nitroxide-based. These molecules are able to efficiently transfer the electron polarization to the nuclei through the fundamentally allowed mechanism referred to as cross-effect.[16] In spinning samples, the cross-effect occurs through three separate rotor events.[17],[18] First, the EPR transition of a given radical is saturated by microwave radiation during a microwave event, which occurs when an electron is on resonance with the microwave frequency. This saturation can be then transferred to the second electron during a dipolar event when the two electrons are on resonance with one another. Lastly, a cross-effect event occurs when the rotor reaches a point where the two electrons of the biradical molecule have EPR transitions that are separated in energy by the Larmor frequency of a hyperfine-coupled nuclear spin. At this condition, a cross-effect event can occur involving the simultaneous flip of the two electrons and the nuclear spin, leading to the hyperpolarization of the nuclear spin. This process is allowed to take place in nitroxides because their electron g-anisotropies are similar in magnitude to the ^{1}H Larmor frequency.[16]

Since the seminal work of Hu and co-workers,[19] who demonstrated that the efficiency of the cross-effect could be greatly improved by tethering two nitroxides together, the development of improved DNP polarizing agents has shown an impressive growth.[20],[21] The first major improvement was in the synthesis of the water-soluble dinitroxide TOTAPol,[22] which is compatible with biological formulations. Matsuki and co-workers subsequently demonstrated that DNP efficiency could be further improved using a rigid linker that fixes the two nitroxides' g tensors in a perpendicular orientation.[23],[24],[25] Zagdoun et al., as well as Sauvée et al., then

showed that the use of large-molecular weight dinitroxides further improves DNP by increasing the electron spin-lattice relaxation times (T_{1e}).[26],[27],[28] The lengthening of T_{1e} can similarly be achieved by deuterating the biradical molecule; however, this also leads to longer DNP build-up times.[29],[30] Recently, Griffin's group has presented trityl-TEMPO biradicals, coined TEMtriPols, in which the trityl radical is most easily saturated due to its low g anisotropy, leading to an improved DNP efficiency, particularly at high magnetic fields.[31],[32]

The most popular polarizing agents currently in use, TEKPol[28] and AMUPol,[27] yield ^{1}H enhancement factors that surpass 200 at a field of 9.4 T, although improved versions of both polarizing agents have been recently presented, offering the enhancement factors that approach the theoretical maximum.[30],[33],[34] Notably, it has also been demonstrated that the TEKPol and AMUPol biradicals are capable of yielding enhancement factors of up to 515 and 363 at 100 K, respectively, in standard solutions that are doped with sapphire crystals.[35] It is thought that the inclusion of these macroparticles locally amplifies the microwaves, thus leading to the greater DNP performance.[35],[36]

Although numerous groups are actively developing improved dinitroxides for DNP applications, the maximum fundamental DNP efficiency of these dinitroxides is unknown and it is unclear whether they can still be meaningfully improved. Synthetic searches for better performing polarizing agents are costly and could be accelerated by proper computational modeling. *In silico* biradical trials could ideally be performed prior to the synthesis of a radical to ensure further progression of the field.

Fittingly, Thurber and Tycko,[17],[18],[37] and Mentink-Vigier et al.,[38],[39],[40] who have developed our modern theoretical understanding of MAS-DNP, as well as Mance et al.[41] have recently developed computational approaches to simulating the MAS-DNP process quantum

mechanically in small spin systems. In principle, these computational tools can be used to predict the efficiency of a given biradical, assuming that its EPR parameters are either known, or can be approximated, with reasonable accuracy.[41] An alternative approach would be to determine the *optimal* EPR parameters belonging to the ideal dinitroxide polarizing agent and to use these results to guide subsequent synthetic work. Here, we demonstrate such an approach, using the software developed by Mance and co-workers[41] to determine the EPR parameters of the hypothetical ideal dinitroxide and estimate how much improvement can be expected from this polarizing agent compared to those currently in use.

Results and Discussion

The software developed by Mance and co-workers[41] calculates the steady-state DNP enhancement of a rotating spin system in Hilbert space. The Hamiltonian describing a three-spin system, consisting of two electrons and a nucleus, experiencing continuous-wave microwave irradiation in a magnetic field can be written as follows:

$$\begin{aligned}\hat{H}(t) = {} & \Delta\omega_{\mathrm{a}}\hat{S}_{\mathrm{az}} + \Delta\omega_{\mathrm{b}}\hat{S}_{\mathrm{bz}} + \omega_{\mathrm{n}}\hat{S}_{\mathrm{nz}} + \omega_{1}\left\{\hat{S}_{\mathrm{ax}} + \hat{S}_{\mathrm{bx}}\right\} \\ & + D\left\{2\hat{S}_{\mathrm{az}}\hat{S}_{\mathrm{bz}} - \hat{S}_{\mathrm{ax}}\hat{S}_{\mathrm{bx}} - \hat{S}_{\mathrm{ay}}\hat{S}_{\mathrm{by}}\right\} + J_{\mathrm{ex}}\left\{2\hat{S}_{\mathrm{az}}\hat{S}_{\mathrm{bz}}\right\} \\ & + \left\{A_{\mathrm{zz}}\hat{S}_{\mathrm{az}}\hat{S}_{\mathrm{nz}} + A_{\mathrm{zx}}\hat{S}_{\mathrm{az}}\hat{S}_{\mathrm{nx}} + A_{\mathrm{zy}}\hat{S}_{\mathrm{az}}\hat{S}_{\mathrm{ny}}\right\}\end{aligned} \qquad (1)$$

In this Hamiltonian, which is defined here in the microwave rotating reference frame, $\Delta\omega_{\mathrm{a,b}}$ corresponds to the difference between the Larmor frequency of the electron labeled a or b and the frequency of the microwave irradiation, with a field strength of ω_1. Note that for dinitroxides, the optimal microwave frequency is known to occur near the g_{yy} tensor component. The electron frequencies are calculated from the g tensor and its orientation in the magnetic field. The orientation of electron b's g tensor is related to that of the first with another set of Euler angles (α, β, γ). ω_{n} is the nuclear Larmor frequency, D and J_{ex} are the electron-electron dipolar and exchange coupling constants, respectively, and A_{ij} describe the electron-nuclear hyperfine

interaction. The relaxation behavior is included by directly relaxing the state populations, in Hilbert space, with rates corresponding to the nuclear and electronic spin-lattice relaxation rates ($f/T_{1e,n}$) where f is the Boltzmann factor. The electron and nuclear coherences are relaxed with their respective transverse relaxation rates ($1/T_{2e,n}$).

The evolution of the density matrix is calculated, over a single rotor period, by separating the evolution propagator $U(t_R)$ into a large number (M) of short time steps:

$$U(t_R) = U_M U_{M-1} ... U_1 \quad (2)$$

The same propagator is then reused to calculate the density matrix at time Nt_R:

$$U(Nt_R) = \left(U(t_R)\right)^N \quad (3)$$

as well as the steady-state density matrix (N→∞). The nuclear state populations and, consequently, the enhancement factor ($\varepsilon_{calc.}$), are calculated from the density matrix by evaluating the eigenvalue of the $\hat{S}_{nz}$ operator,

$$\varepsilon_{calc.} = \frac{\left\langle \hat{S}_{nz} \right\rangle_{MW\ on}}{\hat{S}_{nz,\,eq}} \quad (4)$$

Note that the equilibrium population is used in the calculation of the enhancement factors which compensates for the presence of depolarization effects that affect experimental DNP measurements.[37],[40]

As is evident from equation 1, numerous factors can influence the efficiency of a given polarizing agent. The magnitude of the g tensors impacts the efficiency of the saturation of the EPR line.[28] The dipolar (D) and exchange (J_{ex}) couplings between the two radicals, as well as the hyperfine coupling between the radical and the nucleus (A_{zz}), mediate the three-spin cross-effect. Lastly, the orientation between the g tensors of the two radicals determines the commonness of the cross-effect events and has a strong impact on the DNP efficiency.[42]

Implicit in the analysis is the fact that the longitudinal relaxation time of the electron (T_{1e}) determines the frequency at which a radical can be saturated. A longer coherence lifetime of this state (T_{2e}) is beneficial to ensure that more molecules participate in both rotor events responsible for cross-effect DNP under MAS conditions.[17],[28]

Luckily, a large nine-parameter optimization does not need to be performed to properly sample the parameter space since many of the parameters are either constant, such as the g tensor magnitudes, or operate during different parts of the rotor period[39],[43] and thus can be probed independently of each other. For example, the relative orientation the two g tensors only affects the timings of the different rotor events while the hyperfine coupling and the D, and J_{ex} values, which are also correlated,[44] affect the amount of polarization that is transferred during the rotor events. These rotor events are very short and thus relaxation has its main influences in between these rotor events. In fact, recent simulations that treat the calculation of the positions of the rotor events, the polarization that is transferred (through the Landau-Zenner formula), and the relaxation during entirely separate time periods reproduce the exact results quantitatively.[43] Additionally, optimizing the hyperfine coupling strength would make no chemical sense since in reality a polarizing agent is tasked with hyperpolarizing a large number of nuclei with vastly different hyperfine coupling constants. Its value can therefore be fixed to 0.08 MHz, corresponding to a spin situated outside the spin diffusion barrier.[41] Lastly, experimental studies have shown that the spin-spin relaxation time T_{2e} reaches a plateau near 2.5 μs in concentrations of relevance to DNP applications[33] and thus only T_{1e} needs to be searched. Consequently, our numerical analysis focuses on optimizing the relative orientation of nitroxides, the inter-radical distance, and the electron spin-lattice relaxation time, T_{1e}.

Optimal Relative Orientation of Nitroxides

We first calculated the DNP enhancement factor ε as a function of the relative orientation of the two nitroxide centers. The previously reported electron relaxation times[41] as well as exchange (43 MHz) and dipolar (53 MHz) coupling strengths[45],[46] from AMUPol were used for the calculation. The g tensor was set to g_{xx} = 2.006, g_{yy} = 2.0021, and g_{zz} = 2.0092, corresponding to a nitroxide spin,[47],[46] and the MAS frequency was fixed at 8 kHz; other experimental parameters used in the simulations are described in Computational Details below. Powder averaging was performed over all three Euler angles using a set of 343 orientations of the g tensor with respect to the laboratory frame. In the calculations, the relative orientation of the two g tensors of the nitroxides is specified by the Euler angles (α, β, γ) using the ZYZ convention.[48] Namely, rotations were first performed along g_{zz} by α, followed by subsequent rotations along the new g_{yy} and g_{zz} directions by β and γ, respectively. Chemically speaking, the z axis of a nitroxide is situated perpendicularly to the plane containing the N and its three substituents, while the x axis is aligned along the N-O bond (see Figure 1). As can also be seen in Figure 1, the 'favored' orientation from the bTbK radical corresponds to $\alpha = \beta = \gamma = 90°$.[23] A number of other orientations are also depicted.

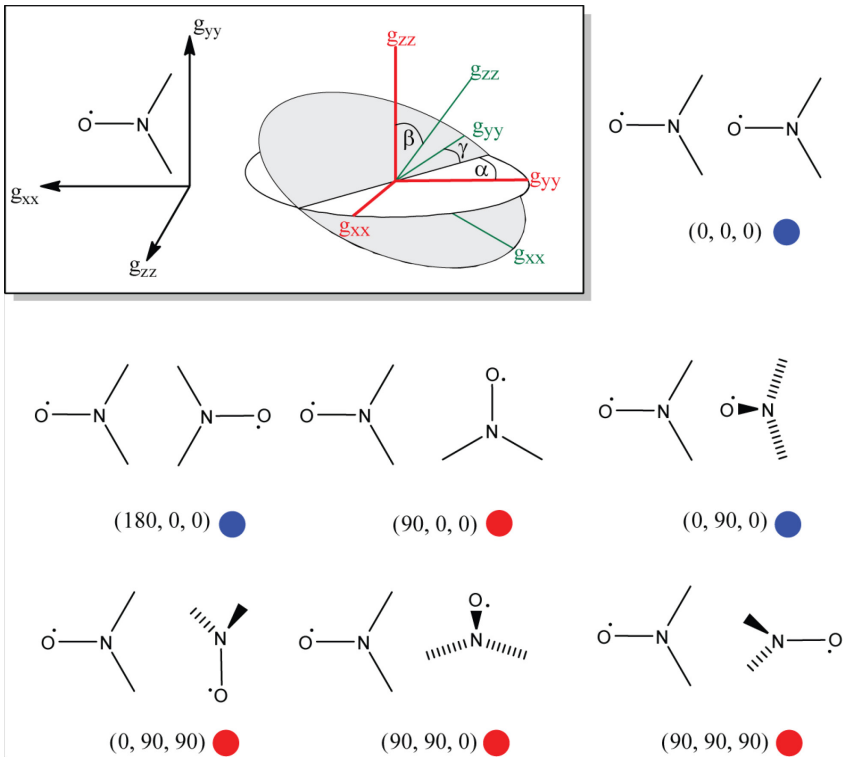

Figure 1. The orientation of the g tensor in the nitroxide molecular frame is shown (top left corner) as well as the coordinate frame defining the three Euler angles. Different biradical orientations are then outlined and their corresponding Euler angle values are listed. Red circles indicate favorable orientations while blue circles indicate disfavorable orientations, *vide infra*.

The predicted steady-state DNP enhancement factor ($\varepsilon_{calc.}$) was calculated as a function of α and β, each of which was incremented in 18° steps from 0° to 180° for γ values of 0°, 30°, 60°, 90°, 120°, and 150°. As anticipated from previous experimental studies,[24] the DNP enhancement varies considerably from <40 to 215 as a function of the relative orientation of the two nitroxides (see Figure 2). Surprisingly, however, the maxima in ε are extremely broad which suggests that a very precise setting of the relative orientation of the two nitroxides is largely unnecessary. Earlier work by Mentink-Vigier suggested that such insensitivity to the g tensor orientations may be found.[39] The improvement in the enhancement factor that can be obtained by further tuning the relative orientation of the two nitroxides from the abovementioned bTbK

orientation[23] is then minimal (< 10%). AMUPol's conformation in solution is unknown and thus it is unclear whether its DNP performance can be improved by altering the orientations of the nitroxide moieties.

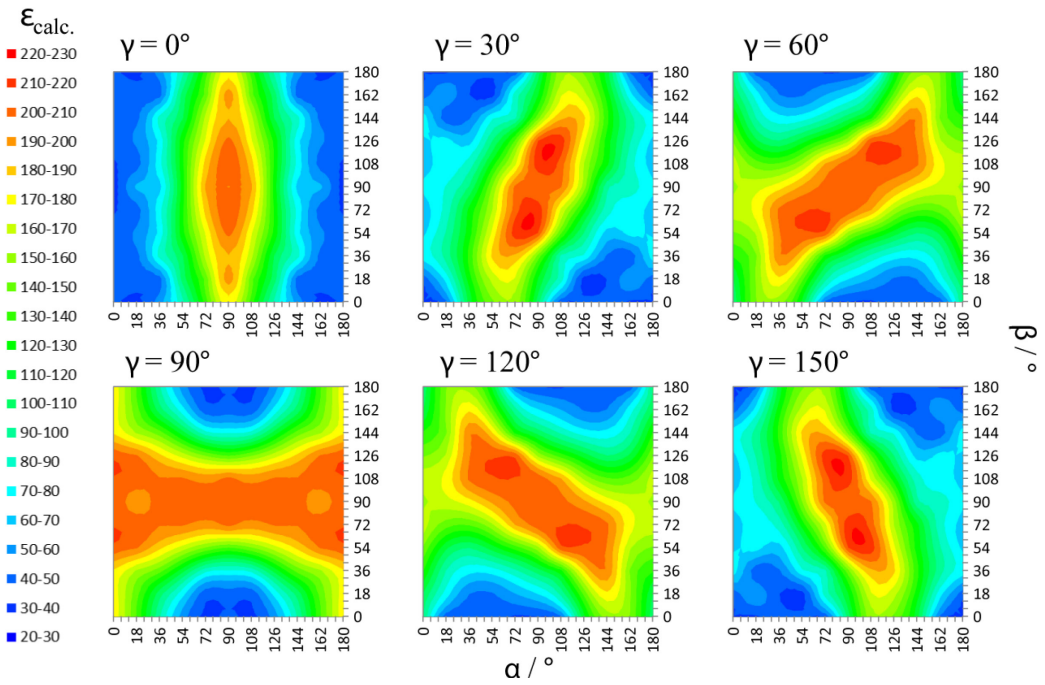

Figure 2. Heat maps of the calculated steady-state DNP enhancement factor ($\varepsilon_{calc.}$) are shown as a function of the Euler angles describing the relative orientation of the two nitroxides' g tensors.

Each plot of the enhancement against α and β (Figure 2) also seems to have its broad maximum crossing at $\alpha = \beta = 90°$ with a slope of approximately: 90°-γ. The existence of such a broad maximum is particularly surprising given that it is believed that the optimal DNP performance will occur when the g_{yy} tensor component of one radical is oriented parallel to g_{zz} of the other.[21],[23],[42] In fact, it appears that the exact orientation of the two radicals' g tensors is irrelevant so long as the g_{yy} components of each nitroxide are oriented perpendicularly to one another. This can be understood, since the microwave irradiation is conventionally applied approximately at the frequency of g_{yy}, for optimal performance, and most orientations where the g_{yy} component of one spin is aligned perpendicularly to the g_{yy} component of the other spin can

satisfy the cross-effect condition by the rotation of the sample. The importance of the perpendicularity of the g_{yy} components is clearly demonstrated by plotting the scalar product of the y unit vector with a rotated y vector ($\vec{y} \cdot \vec{y}_{rot}$, Figure 3). These plots nearly completely reproduce the data from Figure 2, with the exception of the fine structure which originates from the slightly higher, or lower, probability of the cross-effect events occurring for a given orientation.

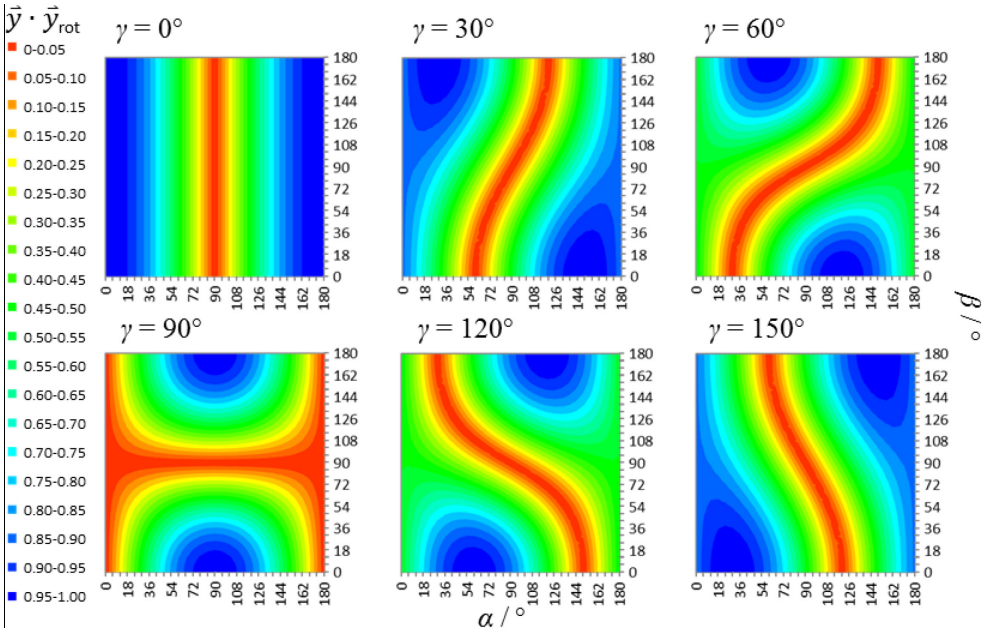

Figure 3. Heat maps of the dot product of the y vector and a rotated y vector are plotted as a function of the Euler angles used for the rotation. It can clearly be seen that these plots closely mirror the calculated data in Figure 2.

Optimal Linker Length

Next we sought to determine the optimal inter-radical distance of TEMPO-based molecules. Although numerous studies have shown that the ε value increases as a function of the dipolar coupling between the radicals,[17],[39],[41] from a chemical standpoint these results are of little use since an increase in dipolar coupling would be accompanied by an exponential increase in exchange coupling.[44] Thus, proper simulations of DNP enhancement factors should

simultaneously include chemically-reasonable exchange coupling constants, which have been experimentally determined for a number of compounds. For example, Kokorin has tabulated typical experimental J_{ex} values as a function of their types of non-conjugated linkers for a number of bis(TEMPO) molecules (Table 1 and Figure 4a),[49] including bTurea (the AMUPol framework).[45] The data show that the size of J_{ex} dominates the dipolar coupling once the linker is three atoms or fewer in length, limiting the impact of further increases in dipolar coupling. Note that the size of J_{ex} depends intimately on the types of atoms in the linker, which can offer a synthetic control over its size.

Table 1. Typical J_{ex} and D values are given for bis(TEMPO) molecules having a different number of linker atoms. Data are summarized from reference 49.

Number of linker atoms	D / MHz[a]	J_{ex} / MHz[b]
1	<100	>1300
2	<65	>220
3[c]	<50	50-400
4	<45	0-140
5[d]	<40	N/A

[a]The dipolar coupling constant is approximated from a typical inter-nitrogen distance assuming no motion; there would of course be some variability depending on the exact linker and the conformation of the molecule; therefore, only an upper limit is given here. [b]Note that the exchange coupling can be remarkably strong over long distances if the linker is conjugated; these linkers are not considered here. [c]AMUPol has 3 linker atoms. [d]TEKPol has 5 linker atoms.

We have calculated the DNP enhancement factor as a function of the number of linker atoms using dipolar coupling constants as well as different values of J_{ex} in the ranges listed in Table 1. These data are tabulated in Table 2. Generally, in agreement with previous theoretical work[39],[46] as well as the experimental work of Mathies and co-workers for TEMTriPols,[32] the highest DNP performance is achieved when the exchange coupling is in the range of 40-100 MHz. It is important to note, however, that these simulations are performed using an applied magnetic field strength of 9.4 T and that the effect of J_{ex} on the DNP performance is expected to

be magnetic field-dependent.[32] In contrast to previous theoretical work which focused on increases in dipolar coupling,[17] we see only a very minor dependence of the enhancement factor on the linker length when exchange coupling is taken into consideration, assuming the optimal J_{ex} value is used for the corresponding linker length (see Figure 4 and Table 2). It is therefore unlikely that any increase in DNP performance could be obtained by further shortening the linker, or by changing its form in the case of AMUPol. Given that that TEKPol is believed to have zero J_{ex},[30] however, it may be possible to improve its performance by modifying the linker in order to increase the exchange coupling to approximately 50 MHz.

Table 2. Calculated DNP enhancement factors as a function of the D and J_{ex} values.

D / MHz	J_{ex} / MHz	$\varepsilon_{calc.}$
40	0	161.2
40	20	135.3
40	40	206.1
40	60	195.1
40	80	189.2
40	100	192.5
45	0	162.1
45	25	194.4
45	50	204.5
45	75	190.4
45	100	181.7
45	125	176.9
50	50	205.5
50	75	191.6
50	100	180.8
50	150	173.8
50	200	146.9
65	200	150.9
65	250	135.3
65	300	93.5
65	400	64.9
65	500	26.5
100	1300	36.9

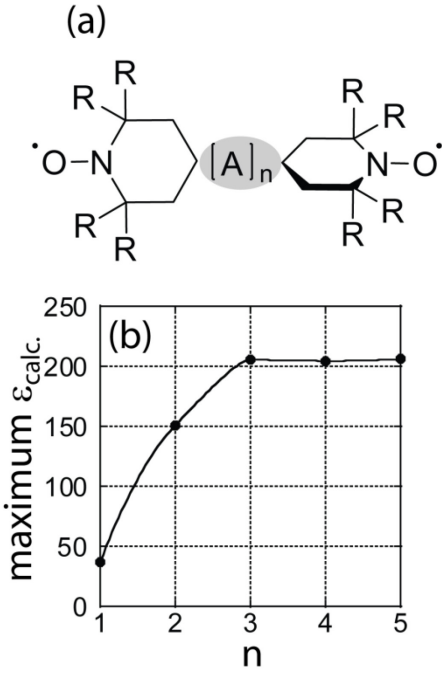

Figure 4. The basic structure of the dinitroxide considered here is shown in (a) where A is a main group element. The length of the linker was varied by changing the number and type of atoms in the linker. A plot showing the highest calculated DNP enhancement as a function of the linker length, expressed by the number of atoms in the chain, n, is shown in (b). In all cases only chemically-reasonable J_{ex} values[49] were used (see Tables 1 and 2). A line is added as a visual guide. α, β, and γ were all set to 90° for these calculations.

Optimal Relaxation Time

The last remaining factors that may influence the performance of a dinitroxide for cross-effect MAS-DNP are the relaxation times of the electrons (T_{1e} and T_{2e}). Researchers are now targeting radicals that are expected to possess increased relaxation times because slower relaxation enables a larger saturation factor to be obtained and increases the fraction of spins that can participate in both rotor events involved in cross-effect DNP. This has been done, for example, by preparing larger, more rigid, biradicals and by isotope labelling.[28],[29]

Zagdoun and co-workers,[28] as well as Sauvée and co-workers,[33] have measured the T_{1e} and T_{2e} values in series of radicals belonging to the bTbK and bTurea families, respectively. Their data show that, when using a 10 mM biradical concentration, the T_{2e} value is correlated to the T_{1e} value at short relaxation times (T_{1e} being c.a. 30 times larger) but that the T_{2e} value reaches a plateau at c.a. 2.5 μs. We have therefore opted for keeping the value of T_{2e} constant (at 2.5 μs) and have calculated the steady-state DNP enhancement factor as a function of T_{1e}, using the same 3-spin quantum model and set of parameters as in the simulations shown earlier in Figure 2, with $\alpha = \beta = \gamma = 90°$.

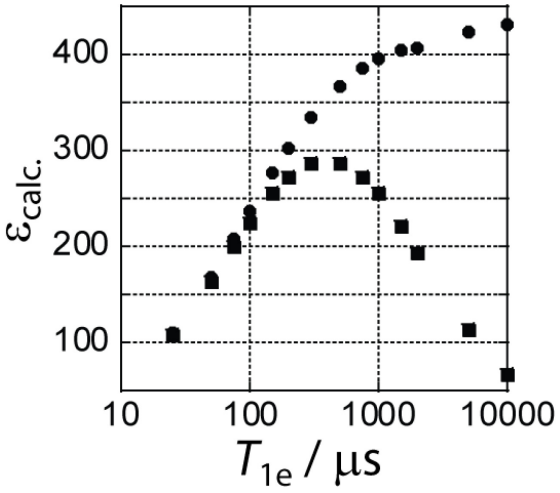

Figure 5. The calculated DNP enhancement factor is plotted as a function of the T_{1e} value. The circles represent the enhancement calculated from the quantum mechanical 3-spin model while the squares are the enhancement factors corrected for the polarization of 1110 nuclear spins per biradical molecule, see text.

As can be seen from the data in Figure 5, as the T_{1e} value is increased, the DNP enhancement factor increases dramatically until a plateau is reached when $T_{1e} > 1$ ms. The absence of a well-defined maximum in this case is a product of the principal approximation used in the simulation model, namely the simple 3-spin quantum mechanical model does not account

for dissipation of ^{1}H polarization in large spin systems. In a real sample, however, each biradical molecule is tasked with hyperpolarizing thousands of nuclear spins. If we consider a 90:10 D_2O:H_2O solution, for example, the ^{1}H concentration is 11.1 M. If we then use a 10 mM biradical concentration, each biradical molecule must then polarize 1110 individual ^{1}H spins, assuming a homogeneous biradical distribution. In contrast to this, however, with 100% quantum yield, only 200 ^{1}H spins can be polarized if the electron T_{1e} value is 10 ms, since the ^{1}H relaxation time in our simulations was set to 2 s.

In order to correct for the fact that each biradical molecule must polarize many spins, we have opted to correct the calculated DNP enhancement factors using a simple kinetic model. If we assume that the radical is continually transferring its polarization (P) to the nuclei, then the polarization transfer rate would be equal to $(T_{1e}N_{spins})^{-1}$, where N_{spins} is the total number of spins that a biradical molecule needs to polarize. Simultaneously, polarization is lost at a rate of $(T_{1n})^{-1}$ through the spin-lattice relaxation of the nuclei. At the steady state ($P(\infty)$), these two processes must have an equal rate:

$$\lim_{t\to\infty}\frac{\partial P(t)}{\partial t} = -\frac{P(t)-1}{T_{1n}} - \frac{P(t)-\varepsilon_{calc.}}{N_{tot}T_{1e}} = 0 \qquad (5)$$

Thus, the corrected calculated DNP enhancement factor is given by:

$$\varepsilon = \frac{T_{1n}\varepsilon_{calc.} + N_{spins}T_{1e}}{T_{1n} + N_{spins}T_{1e}}. \qquad (6)$$

The corrected calculated DNP enhancement factors are also plotted in Figure 5. As can be seen, when the electron relaxation is faster than the nuclear relaxation, the corrected enhancement factors equal those of the 3-spin model while these strongly deviate when the electron T_{1e} is of a similar magnitude to the nuclear relaxation time. The corrected calculated enhancement factors show a clear maximum performance for a T_{1e} of 500 μs, when a radical concentration of 10 mM

is used for a 90:10 D_2O:H_2O solution. Interestingly, Sauvée and co-workers synthesized an AMUPol derivative, named TetraPEG, with a remarkably long T_1e value of 1195 μs.[33] This radical showed a lower DNP efficiency than AMUPol and their best performing biradical, PyPolPEG2OH, which has a T_{1e} value of 691 μs. PyPolPEG2OH is notably the only DNP polarizing agent that has yielded a DNP enhancement factor surpassing 300 without the incorporation of dielectric particles. It is likely that this biradical already has near-optimal relaxation properties for a dinitroxide polarizing agent and that further improvement is impossible. It may nonetheless be possible to further improve TEKPol, which is mostly used in materials science, by lengthening its electron spin-lattice relaxation time.

Instead of the kinetic model presented here, which provides the physical upper limit in hyperpolarization in the presence of relaxation, various groups have applied kinetics-based spin diffusion models to calculate the dissipation of hyperpolarization into a protein,[50] mesoporous material,[51] or microcrystal.[52] Importantly, on the length scales discussed here, spin diffusion distributes the polarization in the solution quite homogeneously. These models tend to reproduce the effects of the finite nuclear relaxation times but assume that the hyperpolarization builds-up instantaneously, which fails to reproduce the effects of electron relaxation. Importantly, however, Mentink-Vigier has very recently applied a similar model, with discrete spins that are hyperpolarized quantum mechanically in real time, in order to simulate the DNP process in systems consisting of hundreds of spins.[43]

Conclusions

We performed an extensive search for the optimal EPR parameters belonging to a biradical polarizing agent. Our simulations focused on optimizing the factors that can be altered by fine-tuning the chemical structure of the polarizing agent such as the orientation of the

radicals, the length of the linker, and the size and rigidity of the molecule (which affects the electron relaxation times). We discovered that the newly synthesized PyPolPEG2OH[33] polarizing agent has nearly-optimal EPR parameters in all of these categories and thus it is unlikely that meaningful improvements over this polarizing agent will be obtained in the future. Research into better performing polarizing agents should then focus on: (1) the synthesis of new polarizing agents having narrow EPR lines, such as trityl radicals[32],[53] and paramagnetic metal centers,[54],[55],[56] and (2) biradical formulations that minimize sample quenching as well as the reactions between the polarizing agent and the material.[57],[58],[59]

Computational Details

All calculations were performed using the software developed by Ivanov and co-workers.[41] All of the reported DNP enhancement factors were calculated at a magnetic field strength of 9.394 T and a temperature of 100 K, with continuous wave irradiation at a frequency of 263.45 GHz with strength of 850 KHz. The sample rotation frequency was set to 8 kHz and the g tensor was fixed to $g_{xx} = 2.006$, $g_{yy} = 2.0021$, and $g_{zz} = 2.0092$. In all cases, the propagator over one rotor cycle was calculated by separating the time evolution into 1 ns increments. For the data presented in Table 2 and Figure 4, this increment was reduced to 100 ps in order to ensure a proper conversion, with rapid oscillations occurring from the larger coupling strengths. In all cases the values of T_{1n} and T_{2n} were set to 2 s and 1 ms while the values of T_{1e} and T_{2e} were set to 50 μs and 0.7 μs, unless stated otherwise. The data shown in Figure 2 were calculated using D and J_{ex} values of 53 and 43 MHz, while subsequent calculations used values of 50 MHz for both. The hyperfine coupling strength was always set to 0.08 MHz, which corresponds to the border of the spin diffusion barrier. In total, of 343 crystal orientations were used for the powder averaging (7 for all three Euler angles).

Acknowledgements

We would like to thank Dr. Konstantin L. Ivanov, Deni Mance, and Prof. Marc Baldus for kindly sharing their code for calculating the DNP enhancement factors. We would also like to thank Dr. Jim Coyle and the HPC team at Iowa State University for their help as well as for giving us access to the CyStorm computer cluster. This research is supported by the U.S. Department of Energy (DOE), Office of Science, Basic Energy Sciences, Division of Chemical Sciences, Geosciences, and Biosciences and the National Science Foundation Engineering Research Center program (EEC-0813570). F. P. was partly supported through a Spedding Fellowship funded by the Laboratory Directed Research and Development (LDRD) program at the Ames Laboratory. Ames Laboratory is operated for the DOE by Iowa State University under Contract No. DE-AC02-07CH11358. F. P. thanks NSERC (Natural Sciences and Engineering Research Council of Canada) and the Government of Canada for a Banting Postdoctoral Fellowship.

References

[1] A. J. Rossini, A. Zagdoun, M. Lelli, A. Lesage, C. Copéret, L. Emsley, *Acc. Chem. Res.* **2013**, *46*, 1942-1951.

[2] T. Kobayashi, F. A. Perras, I. I. Slowing, A. D. Sadow, M. Pruski, *ACS Catal.* **2015**, *5*, 7055-7062.

[3] R. L. Johnson, F. A. Perras, T. Kobayashi, T. J. Schwartz, J. A. Dumesic, B. H. Shanks, M. Pruski, *Chem. Commun.* **2016**, *52*, 1859-1862.

[4] R. P. Sangodkar, B. J. Smith, D. Gajan, A. J. Rossini, L. R. Roberts, G. P. Funkhouser, A. Lesage, L. Emsley, B. F. Chmelka, *J. Am. Chem. Soc.* **2015**, *137*, 8096-8112.

[5] M. L. Hirsch, N. Kalechofsky, A. Belzer, M. Rosay, J. G. Kempf, *J. Am. Chem. Soc.* **2015**, *137*, 8428-8434.

[6] P. Styles, N. F. Soffe, C. A. Scott, D. A. Cragg, F. Row, D. J. White, P. C. J. White, *J. Magn. Reson.* **1984**, *60*, 397-404.

[7] A. W. Overhauser, *Phys. Rev.* **1953**, *92*, 411-415.

[8] T. R. Carver, C. P. Slichter, *Phys. Rev.* **1953**, *92*, 212-213.

[9] J. H. Ardenkjaer-Larsen, B. Fridlund, A. Gram, G. Hansson, L. Hansson, M. H. Lerche, R. Servin, M. Thaning, K. Golman, *Proc. Natl. Acad. Sci. USA* **2003**, *100*, 10158-10163.

[10] T. Maly, G. T. Debelouchina, V. S. Bajaj, K.-N. Hu, C.-G. Joo, M. L. Mak-Jurkauskas, J. R. Sirigiri, P. C. A. van der Wel, J. Herzfeld, R. J. Temkin, R. G. Griffin, *J. Chem. Phys.* **2008**, *128*, 052211.

[11] A. Lesage, M. Lelli, D. Gajan, M. A. Caporini, V. Vitzthum, P. Miéville, J. Alauzun, A. Roussey, C. Thieuleux, A. Mehdi, G. Bodenhausen, C. Copéret, L. Emsley, *J. Am. Chem. Soc.* **2010**, *132*, 15459-15461.

[12] A. B. Barnes, G. De Paëpe, P. C. A. van der Wel, K.-N. Hu, C.-G. Joo, V. S. Bajaj, M. L. Mak-Jurkauskas, J. R. Sirigiri, J. Herzfeld, R. J. Temkin, R. G. Griffin, *Appl. Magn. Reson.* **2008**, *34*, 237-263.

[13] Ü. Akbey, H. Oschkinat, *J. Magn. Reson.* **2016**, *269*, 213-224.

[14] L. R. Becerra, G. J. Gerfen, R. J. Temkin, D. J. Singel, R. G. Griffin, *Phys. Rev. Lett.* **1993**, *71*, 3561-3564.

[15] M. Rosay, L. Tometich, S. Pawsey, R. Bader, R. Schauwecker, M. Blank, P. M. Borchard, S. R. Cauffman, K. L. Felch, R. T. Weber, R. J. Temkin, R. G. Griffin, W. E. Maas, *Phys. Chem. Chem. Phys.* **2010**, *12*, 5850-5860.

[16] C. T. Farrar, D. A. Hall, G. J. Gerfen, S. J. Inati, R. G. Griffin, *J. Chem. Phys.* **2001**, *114*, 4922-4933.

[17] K. R. Thurber, R. Tycko, *J. Chem. Phys.* **2012**, *137*, 084508.

[18] K. R. Thurber, R. Tycko, *Isr. J. Chem.* **2014**, *54*, 39-46.

[19] K.-N. Hu, H.-h. Yu, T. M. Swager, R. G. Griffin, *J. Am. Chem. Soc.* **2004**, *126*, 10844-10845.

[20] K.-N. Hu, *Solid State Nucl. Magn. Reson.* **2011**, *40*, 31-41.

[21] C. Ysacco, H. Karoui, G. Casano, F. Le Moigne, S. Combes, A. Rockenbauer, M. Rosay, W. Maas, O. Ouari, P. Tordo, *Appl. Magn. Reson.* **2012**, *43*, 251-261.

[22] C. Song, K.-N. Hu, C.-G. Joo, T. M. Swager, R. G. Griffin, *J. Am. Chem. Soc.* **2006**, *128*, 11385-11390.

[23] Y. Matsuki, T. Maly, O. Ouari, H. Karoui, F. Le Moigne, E. Rizzato, S. Lyubenova, J. Herzfeld, T. Prisner, P. Tordo, R. G. Griffin, *Angew. Chem. Int. Ed.* **2009**, *48*, 4996-5000.

[24] E. L. Dane, B. Corzilius, E. Rizzato, P. Stocker, T. Maly, A. A. Smith, R. G. Griffin, O. Ouari, P. Tordo, T. M. Swager, *J. Org. Chem.* **2012**, *77*, 1789-1797.

[25] M. K. Kiesewetter, B. Corzilius, A. A. Smith, R. G. Griffin, T. M. Swager, *J. Am. Chem. Soc.* **2012**, *134*, 4537-4540.

[26] A. Zagdoun, G. Casano, O. Ouari, G. Lapadula, A. J. Rossini, M. Lelli, M. Baffert, D. Gajan, L. Veyre, W. E. Maas, M. Rosay, R. T. Weber, C. Thieuleux, C. Coperet, A. Lesage, P. Tordo, L. Emsley, *J. Am. Chem. Soc.* **2012**, *134*, 2284-2291.

[27] C. Sauvée, M. Rosay, G. Casano, F. Aussenac, R. T. Weber, O. Ouari, P. Tordo, *Angew. Chem. Int. Ed.* **2013**, *52*, 10858-10861.

[28] A. Zagdoun, G. Casano, O. Ouari, M. Schwarzwälder, A. J. Rossini, F. Aussenac, M. Yulikov, G. Jeschke, C. Copéret, A. Lesage, P. Tordo, L. Emsley, *J. Am. Chem. Soc.* **2013**, *135*, 12790-12797.

[29] F. A. Perras, R. R. Reinig, I. I. Slowing, A. D. Sadow, M. Pruski, *Phys. Chem. Chem. Phys.* **2016**, *18*, 65-69.

[30] D. J. Kubicki, G. Casano, M. Schwarzwälder, S. Abel, C. Sauvée, K. Ganesan, M. Yulikov, A. J. Rossini, G. Jeschke, C. Copéret, A. Lesage, P. Tordo, O. Ouari, L. Emsley, *Chem. Sci.* **2016**, *7*, 550-558.

[31] K.-N. Hu, V. S. Bajaj, M. Rosay, R. G. Griffin, *J. Chem. Phys.* **2007**, *126*, 044512.

32 G. Mathies, M. A. Caporini, V. K. Michaelis, Y. Liu, K.-N. Hu, D. Mance, J. L. Zweier, M. Rosay, M. Baldus, R. G. Griffin, *Angew. Chem. Int. Ed.* **2015**, *54*, 11770-11774.

[33] C. Sauvée, G. Casano, S. Abel, A. Rockenbauer, D. Akhmetzyanov, H. Karoui, D. Siri, F. Aussenac, W. Maas, R. T. Weber, T. Prisner, M. Rosay, P. Tordo, O. Ouari, *Chem. Eur. J.* **2016**, *22*, 5598-5606.

[34] A. P. Jagtap, M.-A. Geiger, D. Stöppler, M. Orwick-Rydmark, H. Oschkinat, S. T. Sigurdsson, *Chem. Commun.* **2016**, *52*, 7020-7023.

[35] D. J. Kubicki, A. J. Rossini, A. Purea, A. Zagdoun, O. Ouari, P. Tordo, F. Engelke, A. Lesage, L. Emsley, *J. Am. Chem. Soc.* **2014**, *136*, 15711-15718.

[36] F. A. Perras, T. Kobayashi, M. Pruski, *J. Magn. Reson.* **2016**, *264*, 125-130.

[37] K. R. Thurber, R. Tycko, *J. Chem. Phys.* **2014**, *140*, 184201.

[38] F. Mentink-Vigier, Ü. Akbey, Y. Hovav, S. Vega, H. Oschkinat, A. Feintuch, *J. Magn. Reson.* **2012**, *224*, 13-21.

[39] F. Mentink-Vigier, Ü. Akbey, H. Oschkinat, S. Vega, A. Feintuch, *J. Magn. Reson.* **2015**, *258*, 102-120.

[40] F. Mentink-Vigier, S. Paul, D. Lee, A. Feintuch, S. Hediger, S. Vega, G. De Paëpe, *Phys. Chem. Chem. Phys.* **2015**, *17*, 21824-21836.

[41] D. Mance, P. Gast, M. Huber, M. Baldus, K. L. Ivanov, *J. Chem. Phys.* **2015**, *142*, 234201.

[42] K.-N. Hu, C. Song, H.-h. Yu, T. M. Swager, R. G. Griffin, *J. Chem. Phys.* **2008**, *128*, 052302.

[43] F. Mentink-Vigier, S. Vega, G. De Paëpe, *Phys. Chem. Chem. Phys.* **2017**, *19*, 3506-3522.

[44] K. Yamaguchi, M. Okumura, J. Maki, T. Noro, H. Namimoto, M. Nakano, T. Fueno, K. Nakasuji, *Chem. Phys. Lett.* **1992**, *190*, 353-360.

[45] E. K. Metzner, L. J. Libertini, M. Calvin, *J. Am. Chem. Soc.* **1974**, *96*, 6515-6516.

[46] P. Gast, D. Mance, E. Zurlo, K. L. Ivanov, M. Baldus, M. Huber, *Phys. Chem. Chem. Phys.* **2017**, *19*, 3777-3781.

[47] J. S. Hwang, R. P. Mason, L.-P. Hwang, J. H. Freed, *J. Phys. Chem* **1975**, *79*, 489-511.

[48] K. Narita, J.-I. Umeda, H. Kusumoto, *J. Chem. Phys.* **1966**, *44*, 2719-2723.

[49] A. I. Kokorin, *Appl. Magn. Reson.* **2004**, *26*, 253-274.

[50] P. C. A. van der Wel, K.-N. Hu, J. Lewandowski, R. G. Griffin, *J. Am. Chem. Soc.* **2006**, *128*, 10840-10846.

[51] O. Lafon, A. S. l. Thankamony, T. Kobayashi, D. Carnevale, V. Vitzthum, I. I. Slowing, K. Kandel, H. Vezin, J.-P. Amoureux, G. Bodenhausen, M. Pruski, *J. Phys. Chem. C* **2013**, *117*, 1375-1382.

[52] A. J. Rossini, A. Zagdoun, F. Hegner, M. Schwarzwälder, D. Gajan, C. Copéret, A. Lesage, L. Emsley, *J. Am. Chem. Soc.* **2012**, *134*, 16899-16908.

[53] T. V. Can, M. A. Caporini, F. Mentink-Vigier, B. Corzilius, J. J. Walish, M. Rosay, W. E. Maas, M. Baldus, S. Vega, T. M. Swager, R. G. Griffin, *J. Chem. Phys.* **2014**, *141*, 064202.

[54] B. Corzilius, A. A. Smith, A. B. Barnes, C. Luchinat, I. Bertini, R. G. Griffin, *J. Am. Chem. Soc.* **2011**, *133*, 5648-5651.

[55] B. Corzilius, V. K. Michaelis, S. A. Penzel, E. Ravera, A. A. Smith, C. Luchinat, R. G. Griffin, *J. Am. Chem. Soc.* **2014**, *136*, 11716-11727.

[56] B. Corzilius, *Phys. Chem. Chem. Phys.* **2016**, *18*, 27190-27204.

[57] W. R. Gunther, V. K. Michaelis, M. A. Caporini, R. G. Griffin, Y. Román-Leshkov, *J. Am. Chem. Soc.* **2014**, *136*, 6219-6222.

[58] E. Pump, J. Viger-Gravel, E. Abou-Hamad, M. K. Samantaray, B. Hamzaoui, A. Gurinov, D. H. Anjum, D. Gajan, A. Lesage, A. Bendjeriou-Sedjerari, L. Emsley, J.-M. Basset, *Chem. Sci.* **2017**, *8*, 284-290.

[59] W.-C. Liao, T.-C. Ong, D. Gajan, F. Bernada, C. Sauvée, M. Yulikov, M. Pucino, R. Schowner, M. Schwarzwälder, M. R. Buchmeiser, G. Jeschke, P. Tordo, O. Ouari, A. Lesage, L. Emsley, C. Copéret, *Chem. Sci.* **2017**, *8*, 416-422.

Table of Contents Entry

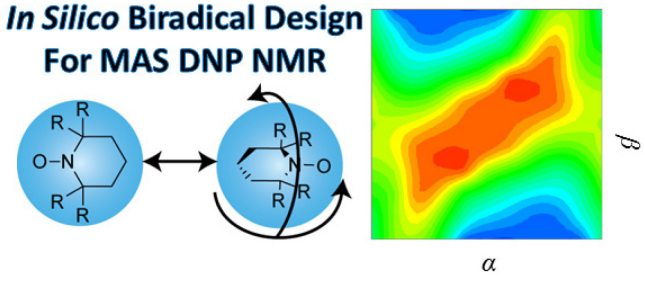

What is the best dinitroxide? Extensive calculations of MAS DNP enhancements are performed as a function of the geometry and relaxation properties of a dinitroxide. The parameters for the "optimal" dinitroxide and determined and the impact these results have on the design of next-generation polarizing agents are discussed.